

Acoustic Function of Sound Hole Design in Musical Instruments

by

Hadi Tavakoli Nia

Submitted to the Department of Mechanical Engineering
in partial fulfillment of the requirements for the degree of

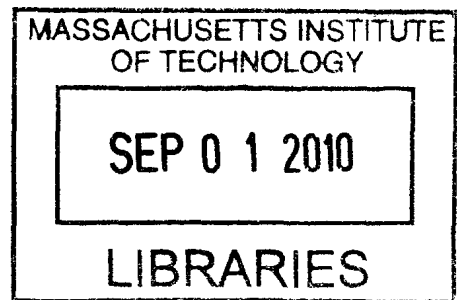
Master of Science in Mechanical Engineering

at the


MASSACHUSETTS INSTITUTE OF TECHNOLOGY

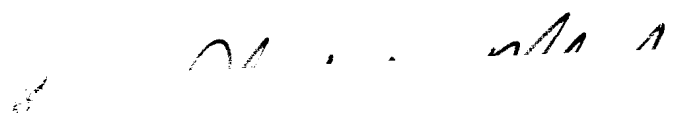
June 2010

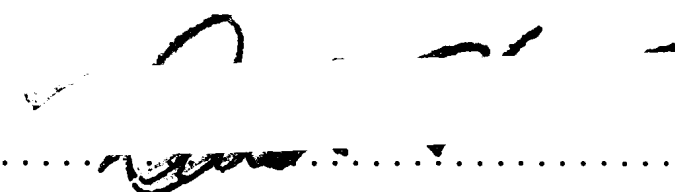
ARCHIVES



© Massachusetts Institute of Technology 2010. All rights reserved.

Author 
Department of Mechanical Engineering
May 22, 2010

Certified by 
Nicholas C. Makris
Professor
Thesis Supervisor

Accepted by 
David E. Hardt
Chairman, Department Committee on Graduate Theses

Chapter 3

Experimental Setup

The experimental setup comprises of a resonance box with variable volume and replaceable top plate. The resonance box is made of a thick cardboard cylinder with changeable diameter and height, confined with top and back plates (Fig. A-3). In order to place the natural frequencies of the box much higher than the air resonance frequencies the walls of the resonance box are chosen from thick 7-mm plywoods and 5-mm cardboards. Sound-holes geometries to be studied are carved in a plywood with thickness 3 mm and are placed on the top plate (Fig. A-4). Use of advanced laser-cutting technologies enabled us to carve complex sound-hole geometries such as the lute rosettes. All the laser cutting process has been done in Media lab and the workshops of the Architecture department at MIT.

The cavity mode is excited with a speaker (Digital BA735, Boston Acoustics Inc.), placed in the distance of 20 cm from the sound-hole, and the receiver was chosen as a microphone (Olympus ME-15) placed inside the resonance box. The microphone is placed on the back plate inside the resonance box to reduce the ambient noise. Moving the microphone to different locations on the back plate showed no significant change in the measurements as is expected because of the small size of the resonance box (30 cm) compared to the wavelength (150 cm). The speaker distance from the resonance box has been changed from 10 cm to 100 cm. Different orientations of the speaker have also been tried by changing the angle between the speaker and resonance box top plates up to 30 degrees. The change in distance and orientation

of the speaker showed no significant change in the measurements. For distances over 100 cm a reduction in signal to noise ratio has been observed. The input signal was designed as a slowly varying ramp around the resonance frequency of the specific opening. The microphone outputs were analyzed by a computer-based acquisition system. The measurements were made in the time domains, then a Fourier transform was used to obtain the frequency domain spectra. The Fourier spectra were window-averaged with a window width of 1000 samples (The sample frequency of the system is 20000 Hz). The resonance frequency is measured as the mean of the two frequencies at which 3-dB down line cuts the curve, that is $f_0 = (f_1 + f_2)/2$ (Fig. A-5). This method gives a low standard deviation for the peak of the curves symmetric around the resonance peak as is in our case. The tests had been first run in closed spaces where distorted resonance curve (as minor second or third peak) had been observed due the reflection from the walls. In order to eliminate the effect of the room on the resonance patterns [6], all the tests have been run in open area (in Killian court at MIT) where the closest wall is at least 50 m far from the setup (the wavelengths we worked with were below 1 m, which are much less than 50 m, the characteristic length of the open area). The resonance curves we measured in the open area were consequently clean of any distortion because of the long distance of the walls as reflectors from the setup.

To quantify the damping effects, the 3-dB and 10-dB down bandwidth of the pressure squared curve normalized to peak are measured directly from the spectrum (Fig. A-5). The 3-dB bandwidth measurements have been cross validated by another method [21], which measures the amplitude decay of the output when the sound-hole is exposed to tone bursts at the resonance frequencies. After exciting the Helmholtz resonator and then removing the excitation source, the system can be modeled as a free simple damped oscillator ([13]). The pressure inside the box can then be expressed as [13],

$$P(t) = P_0 e^{-\zeta^2 \pi f_0 t} \sin(\sqrt{1 - \zeta^2} 2\pi t + \phi) \quad (3.1)$$

where P_0 is the pressure amplitude, ζ the damping factor, f_0 the resonance frequency and ϕ is a phase angle. The following relation holds between the damping factor ζ and the 3-dB bandwidth Δf [19]:

$$\Delta f = 2\zeta f \quad (3.2)$$

So, by measuring the rate of the decay of the pressure oscillation inside the box, we can find a different way to calculate the 3-dB bandwidth Δf . The rate of the decay is obtained by measuring the slope of the decay of $\ln(P(t)/P_0)$ as a function of time (see Fig. A-6) where $P_0 = 1$ is a reference pressure. The slope of the decay is independent of the reference pressure P_0 . From Eq. 3.1, this slope is given by the coefficient of t in the exponential term,

$$\alpha = -\zeta 2\pi f_0 \quad (3.3)$$

From Eqs. 3.3 and 3.2 the 3-dB bandwidth, Δf is given by,

$$\Delta f = -\frac{\alpha}{\pi} \quad (3.4)$$

One of the parameters for calculating the air resonance frequency is the cavity volume, which is difficult to measure in instruments with complex sound box such as violin. The cavity volume of the members of the violin family was measured by assuming top and back plates to be flat. By taking picture of each instrument individually at Johnson String Instrument and inserting the picture in AutoCAD software, we measured the area of the top and back plate and the height of the sound box as shown in Fig. A-7. So, the volume of cavity can be found as the product of the obtained area and the height by neglecting the 3D curvature of the top and back plates at this stage. To include the volume change due to 3D curvature of the top and back plate, a correction factor was calculated for a full length violin by filling the instrument with sand and measuring the exact cavity volume (Fig. A-8). The volume of the cavity by flat top and back plates should be multiplied by 1.145 to give the real volume. Due to lack of access to other instruments in the violin family for

the destructive volume measurement by sand, this correction factor has been used for other instruments.

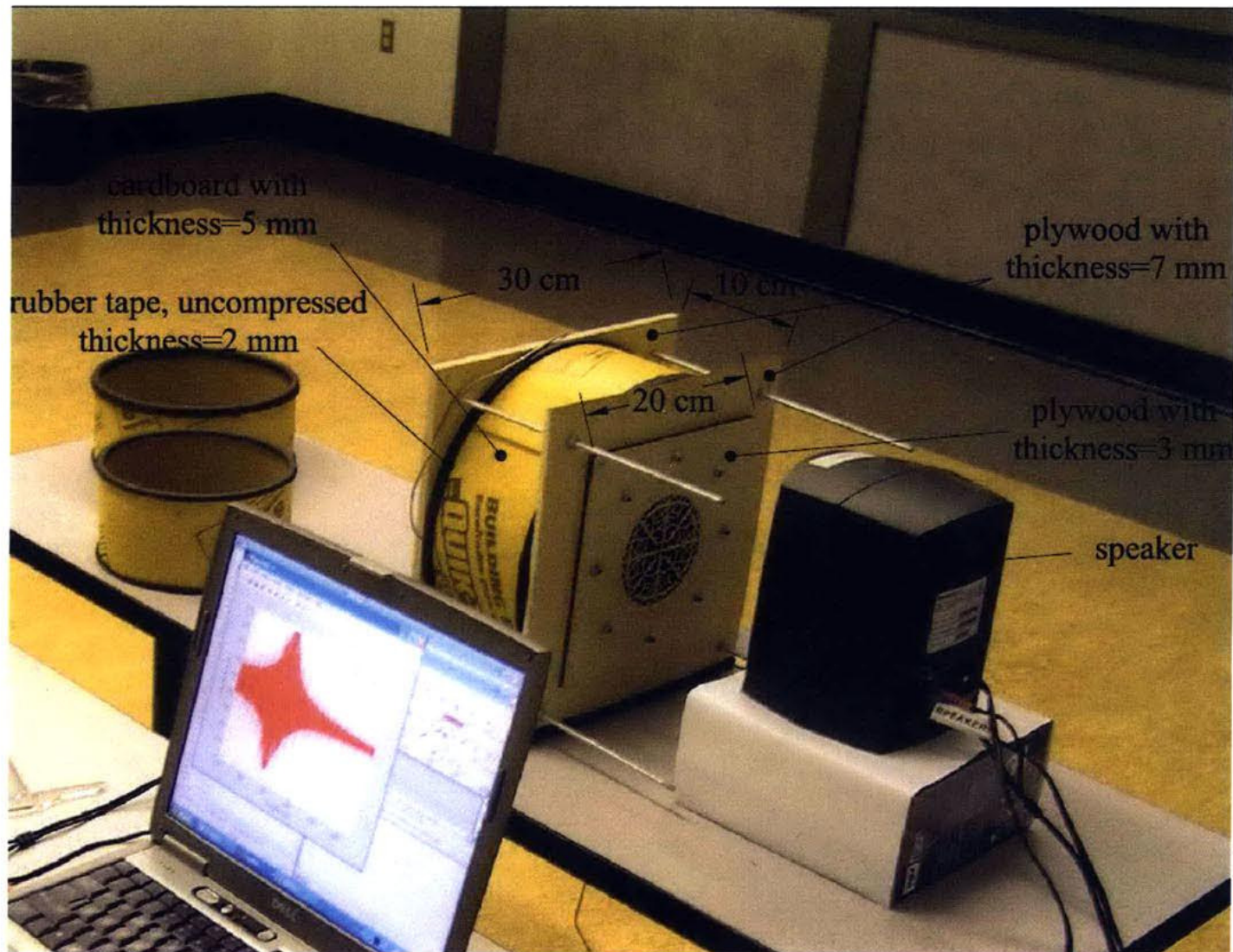


Figure A-3: Resonator setup is shown. The resonance box is made of a cardboard with thickness of 5 mm, and top and back plates out of plywood with thickness of 7 mm. The pattern is carved on a 3-mm plywood and mounted on the top plate. The contact between the top and back plates and the cardboard are sealed with rubber tapes. The microphone as the receiver is placed inside the resonance box attached to the back plate. The speaker is placed in front of the pattern.

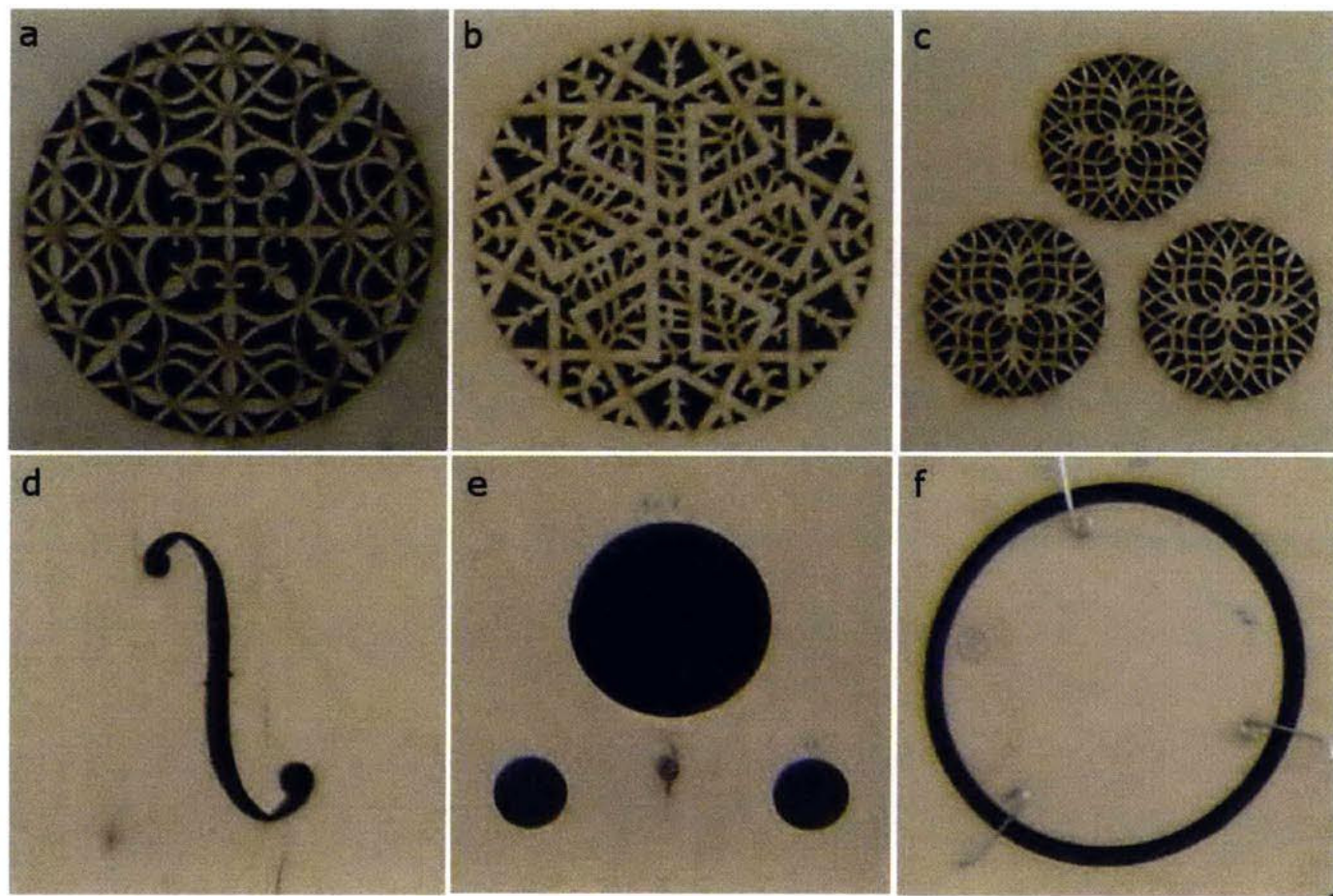


Figure A-4: Opening patterns: (a) Lute rose (Wendelin Tiffenbrucker [1]), (b) Lute rose (Warwick Hans Frei [1]), (c) Theorbo rose [1], (d) Violin f-hole, (e) Oud rose (pattern removed) and (f) sound-hole in the form of a ring.

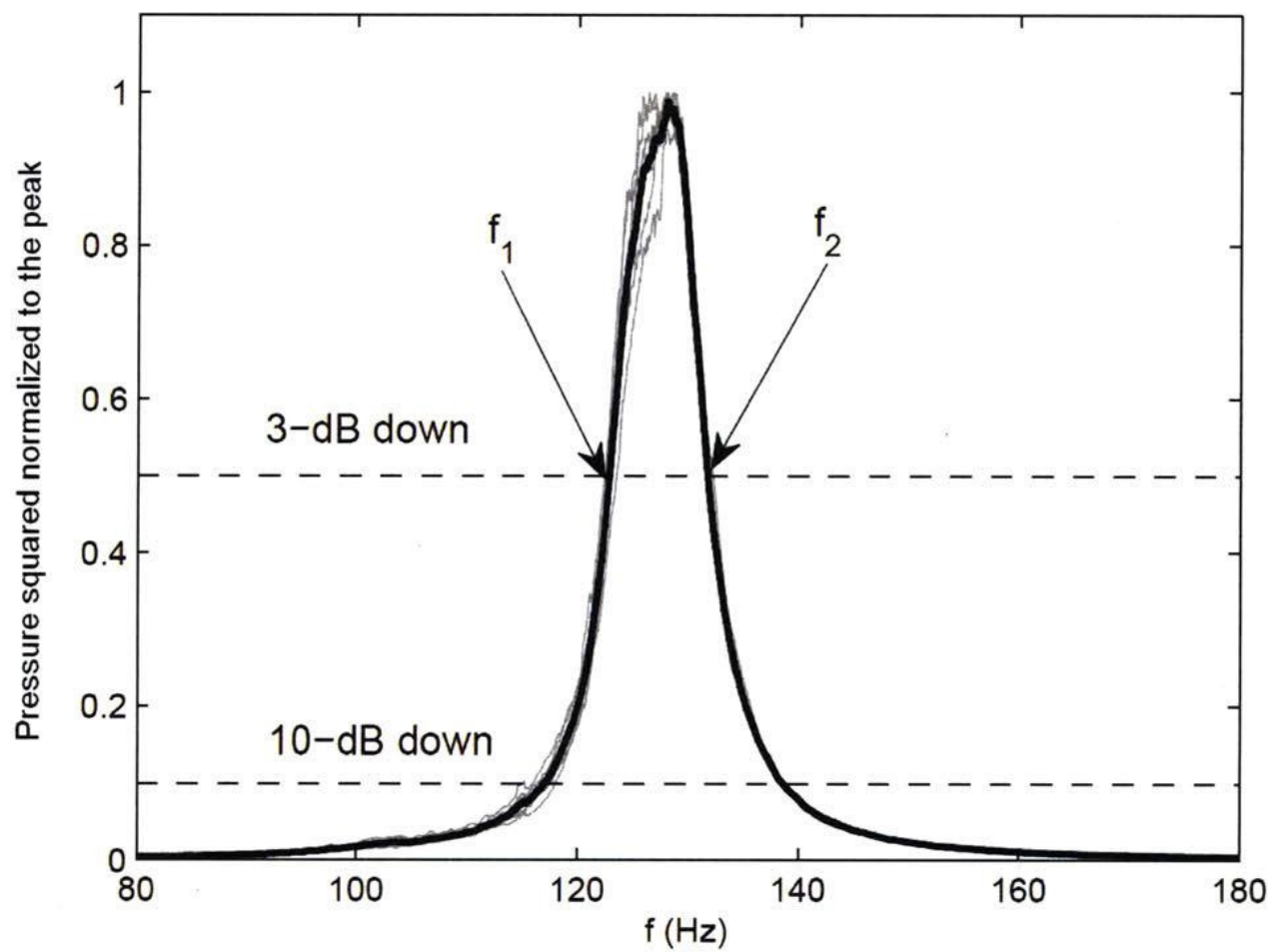


Figure A-5: Air resonance curves of f-hole are shown for $n = 9$ measurements (gray curves). The sound level is normalized by the peak level. Each curve is smoothed by window averaging with window width of 1000 samples. The black line represents the average of the nine measurements. The horizontal dotted line represents the 3-dB and 10-dB down level from the peak. Frequencies f_1 and f_2 are where the 3-dB down level cuts the curve. The peak frequency is then obtained as $f_0 = (f_1 + f_2)/2$.

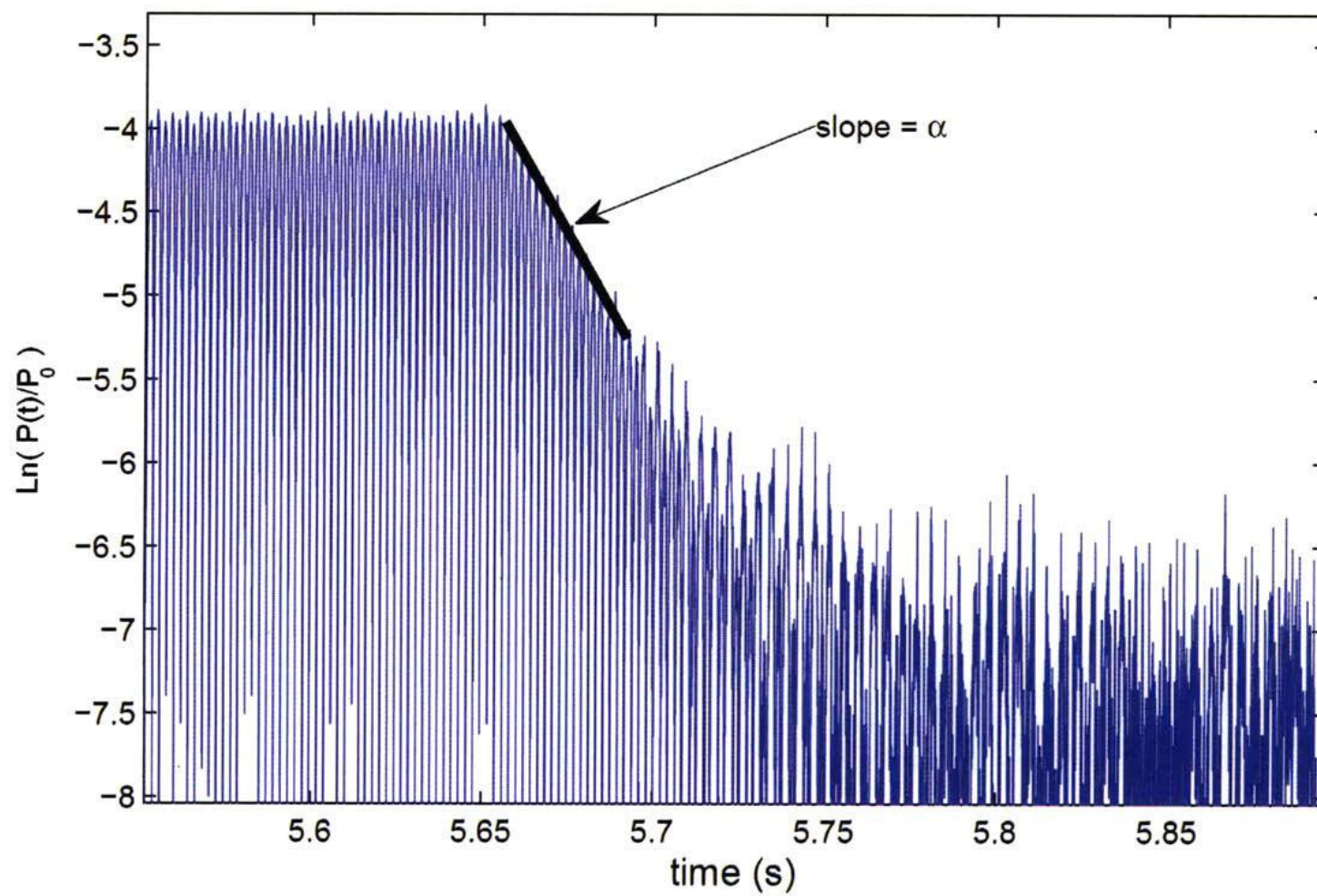


Figure A-6: Measuring the decay slope of the amplitude of the pressure inside the box provides a different method to calculate the 3-dB down bandwidth of the resonance curve shown in Fig. A-5. The slope α is measured during the free oscillation of the resonator after the excitation source is removed (in this figure, after 5.65 s). The 3-dB down bandwidth Δf is then obtained as $\Delta f = -\frac{\alpha}{\pi}$. The reference pressure P_0 is set to $P_0 = 1$. The slope α is independent of the value of P_0 .

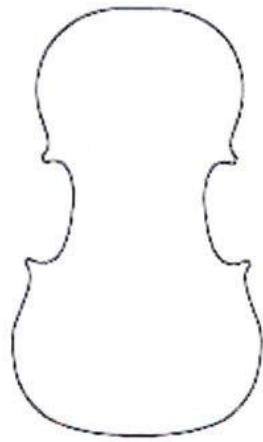
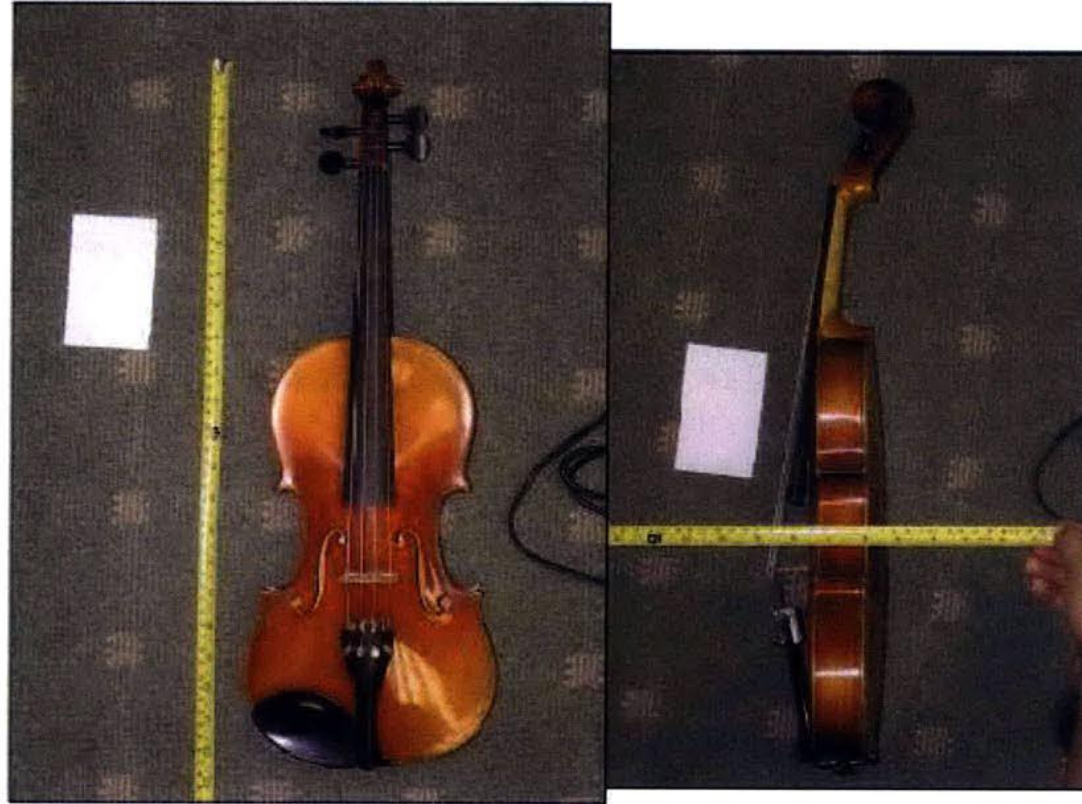


Figure A-7: The volume of the sound box is measured by first assuming the top and back plates to be flat and then correct this assumption by a correction factor obtained by filling the volume with sand. The flat area of the top and back plate and the height of the box is measured in AutoCAD by inserting the images of each instruments.



Figure A-8: The cavity volume is measured by filling the violin with sand.

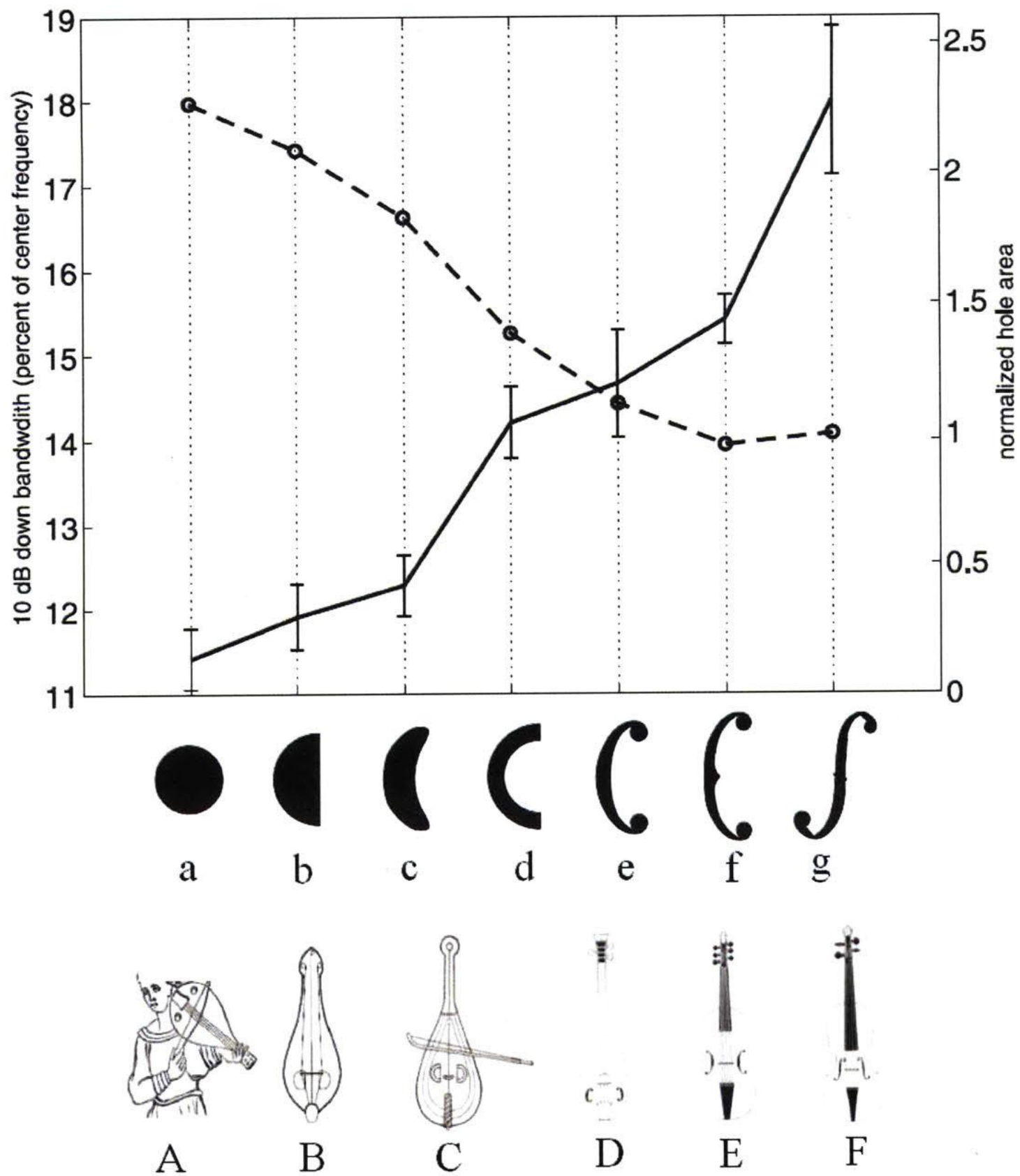


Figure A-16: The line of development of sound-holes in violin is shown for circular opening (a) in 10th-century viols [8] (A), semi-circular opening (b) in Lyras in 13th century [8] (B), crescent (c) [16] and semi-circular strip (d) [20] in 13th century instruments (C), primary c-hole (e) [20] [20] and c-hole (f) in early viols and violins (D,E) in 16th century [5] and present-day f-hole (g) in violins (F) staying unchanged since 17th century [5]. The 10-dB down bandwidths of air resonance of the above openings are shown for a fixed resonance frequency (solid line). The 10-dB-down bandwidth of resonance curve increases monotonically from circular opening to f-hole up to a semitone. The opening area (dotted line), normalized by the area of the present-day f-hole, is reduced by a factor of two from circular opening to c-hole and f-hole.